THE ACCELERATING FLYWHEEL

Dr. David G. Ullman
Department of Mechanical Engineering
Union College
Schenectady, New York 12308
Member ASME

John Corey
Mechanical Technology Incorporated (MTI)
Latham, New York
(Formerly with Union College)
Member ASME

ABSTRACT

A flywheel energy storage unit which can accelerate inertial loads from rest without an external transmission has been designed, built and tested. The preliminary development of this flywheel, a configuration of Band Type Variable Inertia Flywheel (BVIF), is presented. This includes a development of the equations of motion which governs the BVIF mechanism, the properties of a BVIF powering an inertial load, and the design and testing of a prototype model. It will be shown that the BVIF is an energy storage system capable of smoothly accelerating inertial loads to an even terminal speed.

VARIABLE LIST

b band width
E energy
h band thickness
I polar moment of inertia
L single band length
m mass
n number of bands
P power
r_1 hub radius
r_2 outer radius of material wrapped around the hub
r_3 inner radius of material in outer casing
r_4 inner radius of out casing
r_5 outer radius of casing
T torque
Θ angular position
ρ mass density
ω angular speed

Subscripts

B band
eff effective
fixed nonvariable
i inner hub shaft
I moment of inertia
o outer casing shaft
ω angular rate
L load

INTRODUCTION

Many of the end uses of energy depend on its availability in mechanical form, usually as rotating shaft power. Consequently, great advantage would be had in terms of simplicity and overall system efficiencies if energy for such uses could be stored in a rotating mass. Such a device is by definition a flywheel, one of the oldest and most commonly used energy storage mechanisms.

Nonetheless, the uses of flywheels to date have been largely limited to reducing variations in the speeds of shafts driven by pulsed or irregular inputs or supplying peak forces in machine tools such as punch presses. The reason for this underutilization is an inherent difficulty in the power delivery capabilities of conventional flywheels. Specifically, the energy content, E, of a flywheel is a function of the polar moment of inertia, I, and the angular velocity, ω, ($E = \frac{1}{2}I\omega^2$), where the moment of inertia is a function of the mass and the effective radius of that mass from the axis of rotation ($I = \int_m r^2 dm$). For a fixed-inertia system such as the common rotating disk flywheel, then, the energy equation

prescribes reduction in angular velocity as the only means of extracting energy. Most shaft loads, however, require a constant or increasing speed for their operation, so the only means of connecting a fixed-inertia flywheel to such loads is through some type of continuously variable transmission (CVT) or its electrical analog, a motor-generator system. The addition of such a unit to the system usually produces reduction in efficiency and increases in system complexity, weight, and cost. The design and development of effective flywheel energy transmission systems must precede any significant usage of flywheels as energy storage systems.

The flywheel described in this report releases energy in a manner intended to eliminate the need for a CVT or motor-generator by uncoupling the flywheel's energy content from its angular velocity. It is a variable-inertia flywheel (VIF), in which the moment of inertia term I, of the energy equation becomes a variable, allowing net energy release even if the speed term, ω, is constant or accelerating. For the flywheel under consideration here, the mechanism is a coiled thin band wound between an inner hub rotating with angular velocity ω_i and a concentric cylindrical outer casing rotating with angular velocity ω_o. Thus the BVIF is a two-degree-of-freedom device. The layout is much like the installation of a clockwork's mainspring except that no springiness is intended or assumed. As shown in Fig. 1 there are two inter-wound bands for balance but there could be more if desired. Variation in the moment of inertia is accomplished by relative rotation of hub and casing which winds the band material in onto the hub or out against the casing. This device is referred to as the Band-Type Variable Inertia Flywheel (BVIF). Figure 1 also defines the conventions used in all the ensuring discussion. The positive directions for all angular rates and torques are taken to be positive in the counter-clockwise direction shown. The subscripts used for these quantities are: "i" when referring to the inner hub, the inner rotating element, "o" when referring to the casing, the outer rotating element. The torques on hub and casing are due to the band segment between the tightly wound material about the inner hub and that pressed by centrifugal forces in the outer casing. This segment of the band is in tension. The bands exert a positive torque on the hub and a negative torque on the casing when wrapped in the direction shown. The band-wrap direction is defined to be positive when $\omega_o > \omega_i$ causes the bands to accumulate on the hub; negative if $\omega_o > \omega_i$ causes the bands to move out to the casing.

The development history of the BVIF leading to the research reported here is presented in References 1-4. Reference 1 presents an introduction to the variable inertia concept, discusses many potential configurations and studies one configured like a flyball governor. Reference 2 is a digested version of Reference 1. In Reference 3 the Band Type Variable Inertia Flywheel is initially studied. Its equations of motion are derived and three potential ways of connecting it to external systems are developed. These three are as shown in Fig. 2 as Type I, the inner hub connected to the load and the outer casing free; Type II, the inner and outer elements geared together reducing the BVIF to a one-degree-of-freedom system; and Type III, the inner hub, outer casing and load are connected to the three elements of a planetary gear set. In Reference 3 the Type II system was studied and found to be able to power a friction load at near constant speed but not have good inertia load powering capabilities.

This paper is a synopsis of research reported on in Reference 4 where the Type III BVIF, the one with the planetary gear set, has been more deeply studied. The operation of this system is explained by derivation of the equations of motion and their application to the Type III system. A comparison of computer simulation results to experimental data is offered as verification of the equations.

THE BVIF EQUATIONS OF MOTION

The equations of motion of the BVIF (regardless of which Type system) have been derived using Lagragian techniques in References 3 and 4. In Reference 4 the approach is made both through kinetic energy and separately through potenital energy formulations. This dual approach is intended to gain insight into the complex variations of angular rate, band torque and moments of inertia which characterize the operation of a BVIF. Also in Reference 4, for completeness,

the equations of motion have been derived using the standard Newtonian approach. This latter development is presented here assuming a perfect, no-loss system. This assumption is relaxed in later sections of the paper.

According to Newton's 2nd Law, the sum of the torques on a body must equal the time-rate of change of angular momentum or,

$$\Sigma T = \frac{d}{dt}(I\omega).$$

Visualizing the BVIF as a two degree-of-freedom system, drawing free-body diagrams on inner and outer inertias (see Fig. 3), and summing forces on each provides:

$$T_i + T_B = \frac{d}{dt}(I_i\omega_i), \qquad (1)$$

and

$$T_o - T_B = \frac{d}{dt}(I_o\omega_o). \qquad (2)$$

T_B is the only unevaluated term here. To develop an equation for this band torque in terms of the variables defined in Fig. 1, consider a small mass, dm, in the band and moving from radius r_2 to r_3. A rotation of the inner hub, $d\theta_i$, causes a length of band, $dL = d\theta_i r_2$ to unwind. Since band accumulation between windings is not allowed, a casing rotation equal to $d\theta_i \frac{r_2}{r_3}$ is required to absorb dL from the hub. If θ is defined by

$$\theta = \theta_i - \theta_o,$$

then

$$d\theta = d\theta_i - d\theta_o = d\theta_i - d\theta_i \frac{r_2}{r_3}$$

and

$$\frac{dL}{d\theta} = \frac{d\theta_i r_2}{d\theta_i - d\theta_i \frac{r_2}{r_3}} = \frac{r_2 r_3}{r_3 - r_2}.$$

Now, $dm = nhb\rho dL$, so by substitution and rearrangement,

$$d\theta = \frac{dm}{nbh\rho}\left(\frac{r_3 - r_2}{r_3 r_2}\right).$$

As the torque, T_B, does work (causes an energy change) in the band as it moves through the relative angle θ then

$$E = T_B\theta$$

or

$$dE = T_B d\theta.$$

For the bit of band mass, dm, moving from r_2 to r_3, the change in energy is:

$$dE = \tfrac{1}{2}dm r_3^2\omega_o^2 - \tfrac{1}{2}dm r_2^2\omega_1^2.$$

Combining and rearranging the expressions for dE and $d\theta$ gives

$$T_B = \tfrac{1}{2}nhb\rho\left(\frac{r_2 r_3}{r_3 - r_2}\right)(r_3^2\omega_o^2 - r_2^2\omega_i^2), \qquad (3)$$

this characterizes the band torque in terms of the basic system. From the Reference 3 derivation, the expressions for the other variables used are:

$$I_i = \frac{\pi\rho b}{2}(r_2^4 - r_1^4) + I_{i_{fixed}} \qquad (4a)$$

and

$$I_o = \frac{\pi\rho b}{2}(r_4^4 - r_3^4) + I_{o_{fixed}}, \qquad (4b)$$

so

$$\dot{I}_i = 2\pi\rho b r_2^3\dot{r}_2 \qquad (4c)$$

and

$$\dot{I}_o = -2\pi\rho b r_3^3\dot{r}_3, \qquad (4d)$$

where

$$\dot{r}_2 = \frac{nh}{2\pi}\frac{r_3}{r_3 - r_2}(\omega_o - \omega_i) \qquad (4e)$$

and

$$\dot{r}_3 = \frac{r_2}{r_3}\dot{r}_2. \qquad (4f)$$

The variables r_2, r_3 can be used as macroscopic, observable coordinates for the system motion. They depend on the intrinsic coordinates, θ_i and θ_o according to equations 5,

$$r_2 = \frac{(r_{3_o}^2 - r_{2_o}^2) - [(r_{3_o} - r_{2_o}) + K_s(\theta_i - \theta_o)]^2}{2[(r_{3_o} - r_{2_o}) + K_s(\theta_i - \theta_o)]} \qquad (5a)$$

and

$$r_3 = \frac{(r_{3_o}^2 - r_{2_o}^2) + [(r_{3_o} - r_{2_o}) + K_s(\theta_i - \theta_o)]^2}{2[(r_{3_o} - r_{2_o}) + K_s(\theta_i - \theta_o)]} \qquad (5b)$$

where $K_s = \frac{nh}{2\pi}$ and r_{2_o}, r_{3_o} are the values of r_2 and r_3 at time equal to zero.

The above equations constitute a complete modeling of the basic BVIF as a free-standing system with the assumption of perfect, no-loss operation. These factors will be added in the subsequent sections of this paper. Also, from equations 1-5 it is evident that the BVIF is a two degree of freedom system with the angular velocities or positions of the hub and casing as independent coordinates. It is obvious that these equations are highly nonlinear and that the seven independent equations 1, 2, 3, 4a, 4b, 4e and 4f contain 9 unknowns (T_i, T_o, T_B, ω_i, ω_o, I_i, I_o, r_2, r_3). To complete the set of equations the connection of the BVIF to the outside system must be defined.

TYPE III BVIF SYSTEM SIMULATION

The Type III BVIF is by far the most complex dynamically of the BVIF configurations studied to date due to the inclusion of a planetary gear set. However, the complexity offers the most promise for versatility in operation. In this configuration (see Fig. 2), the two shafts of the BVIF (hub and casing) are connected to a load shaft via a planetary (epicyclic gear train) so that at any given time all three shafts can be rotating at different angular rates. The load shaft is notated with the subscript L. The equations of motion do not reduce but rather expand into a set of 11 simultaneous nonlinear equations which can be solved for the torques and accelerations of hub, casing and load shafts. In addition to the seven equations derived earlier there are also additional equations for the load and the planetary gear set. The load torque and angular rate (2 more unknowns) are related by

$$T_L = I_L\dot{\omega}_L + T_F + T_{AERO}\omega_L^2; \qquad (6)$$

where the load is assumed to consist of an inertia I_L, Coulomb friction, T_F, and aerodynamic loss, T_{AERO}. Plus from Reference 5, the torque and rotational relationships for planetary gear sets:

$$T_i = -T_L/(1-gr) \qquad (7a)$$

and

$$T_o = gr \cdot T_L/(1-gr) \qquad (7b)$$

and

$$\dot{\omega}_L = \dot{\omega}_i/(1-gr) - gr\cdot\dot{\omega}_o/(1-gr). \qquad (7c)$$

The gear ratio, gr, is defined as the ratio of θ_i to θ_o when $\theta_L = 0$. Note that the rotation equation (7c) holds for angular position, θ, and angular acceleration, $\dot{\omega}$, as well and that the representation of the gear set in Fig. 2 is purely arbitrary. Any of the elements of the epicyclic train may be attached to the three shafts of the Type III without altering the equations so long as gr is defined as above. Also with the addition of variables T_L and ω_L and equations 6 and 7, there are eleven nonlinear equations and unknowns.

With the planetary gear set in the Type III BVIF it is quite possible to accelerate the load while both hub and casing are slowing down. The acceleration of the load depends on the rate of change in the difference between inner and outer velocities, rather than their absolute values. In fact, for appropriate choices of gr, the load can be made to accelerate positively no matter what the magnitudes or even directions of the two flywheel velocities. In principle a great energy yield may be possible if the flywheel speeds can be brought low while the load shaft speeds up.

TYPE III BVIF - TYPICAL OUTPUT CHARACTERISTICS AND SENSITIVITY TO PARAMETER VARIATION

To demonstrate the output characteristics of a Type III BVIF accelerating inertial load and show the effects of parameter variation a specific example will be used. The dimensions for this example are from the prototype BVIF described in the next section of this paper. The major dimensions for this model are:

r_1 = 0.5 in
r_4 = 5.0 in
n_{band} = 2
h_{band} = .002 in
b_{band} = 1.0 in
L_{band} = 9700 in

$\rho_{steel} = .00073\ lb\cdot s^2/in^4$

$I_{i_{fixed}} = .05\ lb\cdot s^2\cdot in$

$I_{o_{fixed}} = .74\ lb\cdot s^2\cdot in$

$I_{max} = 1.32\ lb\cdot s^2\cdot in\ @\ r_2=.5\ in$

$I_{min} = 0.98\ lb\cdot s^2\cdot in\ @\ r_2=3.5\ in$

The planetary gear set used has a ratio of .75. This value was not selected based on any benefits of this value but because of availability of hardware. In these simulations the entire mechanism is assumed frictionless. Friction effects will be discussed.

In this section the operation of the above dimensioned Type III BVIF will be described in great detail. This will be followed by a discussion of the effect of variation of some of the major dimensions and initial conditions.

For example the baseline initial conditions used are $\omega_i = \omega_o = 500$ rad/sec (4775 rpm) and $r_{2_o} = 3.0$ in. The load is purely inertial and $I_L = .20\ lb\cdot s^2\cdot in$. Initially the inertial load is at rest. The simulation of this example is made in three steps. At time zero the entire BVIF is rotating at 500 rad/sec and a clutch between the load and BVIF is disengaged. At time zero-plus the BVIF is allowed to go free so the various shafts can rotate at different speeds which will happen due to centrifugal forces on the bands. At one second the load clutch is engaged taking one second for the BVIF load shaft and the load to reach a nonslip common speed. From two seconds on the BVIF is directly powering the load with no clutch slip or gear change. The results of this simulation are shown in Fig. 4a-f and 5.

The angular rate time history of the BVIF is shown in Fig. 4 along with the band position r_2. For the first second of the run the BVIF is free so centrifugal force is driving the band material outward ($\dot{r}_2<0$). This causes the inner hub to accelerate due to loss of mass and the casing to decelerate as it gains mass. The load shaft having low inertia speeds up in response to the torques on it through the planetary. Between one and two seconds the clutch is engaged slowing the load shaft. The 190 rad/sec shown for ω_L at two seconds is the speed of the load shaft and the load itself at that time. Prior to one second the load was at rest and with the torque supplied through the slipping clutch accelerated from 0 to 190 rad/sec in the one second interval. From the two second point on the load is accelerated with no clutch slip. To do this $\omega_i<\omega_o$ so the band winds in, $\dot{r}_2>0$. At 8 seconds $\omega_L = \omega_i = \omega_o$ and $\dot{r}_2 = 0$. From this time onward $\omega_o > \omega_i$ and the band winds out into the casing, $\dot{r}_2<0$. This continues until the band is fully out wound. At this time $\omega_L = 800$ rad/sec and the inertial load has been smoothly accelerated from rest with only an initial clutching.

In Fig. 4b the moments of inertia of the system are plotted. Here the moment of inertia of the material rotating at speed ω_i, I_i, is seen to increase initially as the band winds in. Then, as the band winds out I_i falls to $I_{i_{fixed}}$. Similarly the moment of inertia of the material rotating at ω_o, I_o, drops initially then increases steadily. The moment of inertia of the BVIF as seen by the load itself is called the effective moment of inertia, I_{eff}. This ficticious inertia represents the entire BVIF as if all the elements were rotating with angular velocity ω_L. The effective moment of inertia can be derived either by considering the equations of motion which is quite lengthy or by treating the BVIF as a black box so that

$$T_L = \frac{d}{dt}(I_{eff}\omega_L)$$

and solving for I_{eff}. This latter treatment has been used in the computer simulations. As seen in Fig.4b, I_{eff} drops steeply during the high acceleration portion of the run then levels off as the terminal velocity is reached. Essentially the entire system of BVIF plus load must conserve angular momentum so

$$\frac{d}{dt}[(I_{eff} + I_L)\omega_L] = 0$$

or

$$\dot{I}_{eff}\omega_L = -(I_{eff} + I_L)\dot{\omega}_L .$$

Thus $\dot{I}_{eff}$ must be negatively large to give high acceleration to the load in the early portion of the run as can be seen. Figure 4c is the torque-time history of each element of the system. Also included is the history of r_2, or band position. Note that T_B, the band torque is the overwhelming protion of T_i, justifying the usage of the potential energy/band

tension mode of energy removal rather than relying on the inertial change effects to produce usable torque. Note also that all the torques can be approximated as being proportional to r_2. This supports the decision to use in-wound band as the initial condition, in order that the torque curves would have the early peak and trailing long-term response.

Figures 4d, e and f along with Fig. 5 show the power flow within the system. In Fig. 4d the power flow through the planetary is shown. Power P_L is the power given up to the load. P_o is the power transferred to the outer casing through torque T_o. P_i is the power input to the planetary from the hub through torque T_i. As can be seen the sum of these powers equals zero at all times. Power P_i, for example, is derived from the band torque T_B and the rate of change of the energy stored in the mass rotating at speed ω_i. This can be shown as

$$P_i = \frac{d}{dt}E_i + P_B$$

$$= \frac{d}{dt}[\tfrac{1}{2}I_i\omega_i^2] + P_B$$

$$= I_i\omega_i\dot{\omega}_i + \tfrac{1}{2}\omega_i^2\dot{I}_i + P_B \quad .$$

$$= P_{I_\omega} + P_{I_I} + P_B \quad .$$

The first term is due to change in speed and the second due to change in inertia. These two terms and their sum is plotted in Fig. 4e for the inner hub and similarly in 4f for the outer casing. Before discussing the information on these plots Fig. 5 is introduced.

In this figure the various powers from Figs. 4d, e and f are shown in a power flow diagram at selected times. Initially, at time zero, all elements of the BVIF are at the same speed and there is no load thus there is no power flow anywhere within the mechanism. At one second, just prior to clutch engagement, the band is unwinding due to centrifugal force. Thus the inner moment of inertia is dropping, releasing energy but, by conservation of angular momentum the inner hub is accelerating which takes energy. The net effect is that the inner hub is absorbing energy. The opposite is occurring in the outer casing and power is flowing through the band, because of the band torque, from the outer casing to the inner hub. At two seconds the clutch is fully engaged and now there is also power flow through the planetary to the load. The band is winding in (see Fig. 4a) thus $\dot{I}_i$ is increasing, absorbing energy, and both ω_i and ω_o are increasing absorbing energy. However, $\dot{I}_o$ is decreasing at such a high rate as to supply power to the above plus the load (note $P_{I_\omega} + P_{I_I} + P_{o_\omega} + P_{o_I} = -P_L$). As ω_L accelerates ω_o starts to decrease, $\dot{\omega}_o < 0$ as seen at 4 seconds. Now both parameters associated with the outer casing are giving up energy. The same is true at six seconds. Near eight seconds the angular rates become equal and change from $\omega_o > \omega_i$ to $\omega_i > \omega_o$. At this junction the band starts winding out rather than in. Also, at the same time, $\dot{\omega}_i$ is very small. Thus the power terms associated with $\dot{I}_i$, $\dot{I}_o$ and $\dot{\omega}_i$ are all small. From 8 seconds on the band is winding out, thus $\dot{I}_i$ is decreasing and giving up power. However, $\dot{I}_o$ is absorbing power at a faster rate, so the net effect of moment of inertia change is to absorb power. But, the angular speeds are both decreasing at a rate fast enough to overwhelm the inertia effects. In fact, net power is being given up by both segments of the BVIF during the remainder of the run.

In considering at the power flow diagrams one point is noteworthy. Before eight seconds, when the moments of inertia appear to be decreasing, the power flow recirculating through planetary gears and BVIF is on the order of three times what is given up to the load. However, after eight seconds when the apparent moment of inertia is increasing (the effective moment of inertia is still dropping however) the recirculating power is the same order of magnitude as the power to the load. This implies the BVIF is more efficient in its power flow when outwinding.

Based on the simulation presented above and numerous others the effect of changing various parameters on the output will be discussed. There are two sets of parameters, physical measures and initial conditions. The effects of the band thickness, h, and length, L, and number of bands, n are to affect the total amount of band material in the BVIF. In Reference 3 it was shown that the greatest change in moment of inertia was when

$$nLh = \frac{\pi}{2}(r_4^2 - r_1^2) \ .$$

Thus any deviation from this will reduce the available moment of inertia variation potential. The height of the bands, b, and the outer radius of the band casing, r_4, alter the total energy storage capability of the BVIF, the height in direct proportion and the radius as squared. Obviously if r_4 is altered then the band length, thickness or number of bands will need to be altered as discussed above. The hub radius, r_1, has only a weak effect on the design and generally should be kept as small as possible. The band density, ρ, has proportional effect on total energy storage. The band material should be as dense as possible. The fixed inertias, $I_{i_{fixed}}$ and $I_{o_{fixed}}$, reduce the effectiveness of the BVIF. Thus they should be as small as possible.

The effect of the initial speed of the BVIF is to increase the energy stored. The shape of the curves in Fig. 4 do not change other than in time scaling in an inverse proportion. In this example $\omega_{i_o} = \omega_{o_o}$ = 500 rad/sec and the run lasted 30 seconds. If another run was to be made with another initial speed, ω, then the time for the run, t_f, would be

$$t_f = \frac{500 \cdot 30}{\omega} \ .$$

So if ω = 1000 rad/sec then t_f = 15 sec.

The effect of load moment of inertia and of the initial band position as measured by r_{2_o} can best be discussed in terms of Fig. 6. This figure is the result of many simulated runs where the initial band position as measured by r_{2_o} and the inertial load were varied. The approach to the figure can best be seen by example. Say that r_{2_o} = 3.0, most of the material is inwound and I_L = .20 lb·s^2·in, point A in the Figure. When the load is engaged the BVIF will initially wind in the bands until r_2 = 3.5 which is $r_{2_{max}}$. Then the bands will totally unwind into the outer casing. In accomplishing the wind and unwind the BVIF will release 56% of its initial stored energy. This is the same run as presented in Figs. 4 and 5. If I_L = .05 for example the band would not inwind at all, $r_{2_{max}}$ = 3.0 and just outwind until all the band material was in the outer casing. The BVIF would have released only 28% of its stored energy in performing this task.

It is interesting to note that the final speed of a load accelerated from rest is a function of initial speed only. (An exception to this statement is at very low load inertias, .05 lb·s^2·in or less). In general the ratio of final load speed to initial BVIF speed is 1.60 ± 10%. Thus for this case the initial BVIF speed was 500 rad/sec and the final was 795 rad/sec near the 800 rad/sec calculated by the general ratio.

From the above it can be concluded that the Type III BVIF can accelerate a frictionless inertial load irrespective of initial band position, angular rate, or, within bounds, moment of inertia of the load. In actuality the moment of inertia of the load as seen by the BVIF can be modified by fixed ratio gearing as, of course, can the speed of the load. Gearing such as described can only be designed with a specific load in mind. Thus the next step in BVIF development will be the application of the Type III BVIF to a specific load such as a vehicle.

No mention has yet been made about some practical aspects of BVIF design such as dynamic balance and energy density. Balance considerations will be mentioned in the next section. In discussing energy density for the BVIF care must be taken as the BVIF is both the energy storage unit and a major part of the transmission system. However, analysis in Reference 4 has shown that, assuming the outer ring carries the entire centrifugal load of the bands (the band carry none of their own load) and the bands are steel and the outer ring is Kevlar (working stress 130,000 ksi) the energy density is 5.9 watt hr/lb. Left out of this value are the load carrying capacities of the end plates which support the outer ring, the load carrying capacity of the bands themselves and the weight of the end plates, gears, bearings and containment. But, even if 3 watt hr/lb is realizable it still may be acceptable in an era of 40 watt hr/lb fixed inertia flywheels because the BVIF is not only a flywheel but a transmission system as well.

BVIF PROTOTYPE TESTING

In order to verify the dynamic simulation results and gain knowledge of the BVIF's true potential, a prototype model was designed, constructed and tested. The design of the prototype model is based on the proof-of-concept model described in Reference 3. Like the previous version, this prototype is 10½" in diameter and 1 3/8" thick at the rim. The band material occupies a cavity 10" in diameter and 1.05" high. The maximum design rotational rate is 5000 rpm. The stresses resulting from this speed are quite conservative in keeping with the primary design objective of verifying the equations of motion not in producing a high energy density system.

The resulting prototype configuration and its test stand are presented in photographic Figs. 7 and 8. The prototype as seen in Fig. 7 only shows the outside of the casing. Internally, as shown in Fig. 8, the center hub is really a spool to help reduce internal friction. Essentially, the physical properties of this prototype are as used for the simulations in the previous section.

To support the analysis the prototype model was used to accelerated an inertial load. The simulation was modified by the addition of bearing, gear, and windage friction (no vacuum was used). The gear and bearing friction values were measured (Reference 4) and the windage values were empherical (Reference 3). A typical comparison of results is shown in Fig. 9. Here the two measured values, the loadshaft rpm and the inner hub shaft rpm are plotted with simulated values. As can be seen the simulation is always within 10% of the measured values. The effects of the friction can be seen by comparing Figs. 4a and 9. The major features are that the ratio of maximum load speed to initial BVIF speed is lower and the rpm tapers off with time. There was no effort beyond using a good grade of bearings to reduce friction in the prototype testing.

In operating the prototype speeds of up to 3500 rpm were run. At thes speeds there was no apparent problem with balancing. With the use of two bands and the high inertial loads, mass was always symetric about the axis. Potential problems which might be encountered in a moving base application are unknown, but the amount of material mass between the tight wound outer and inner sections of band are very small and, thus, little problem is foreseen.

CONCLUSIONS AND RECOMMENDATIONS

1. The Band-Type Variable Inertia Flywheel (BVIF) is a system capable of storing and delivering energy in usable form. This is a single mechanism, which, unlike conventional flywheels does not require any intermediate transmission equipment. A BVIF has been built and operated which is capable of smoothly accelerating a directly-connected inertial load from rest to a final speed without clutch-slipping losses or any additional transmission devices.

2. There are essentially three ways to attach loads to a BVIF. The first is an open-loop system with two degrees of freedom, referred to as the Type I. The Second (Type II) is a single-degree-of-freedom unit with a fixed ratio between hub speed and casing speed. Third (Type III) has two degrees of freedom like Type I but includes power recirculation through a gear train like Type II. Of these, the Type III has been identified as the most promising configuration.

3. The Type III BVIF is capable of accelerating inertial loads smoothly and with stability to a terminal speed. That final speed can be greater than the initial flywheel speed, and both inner and outer elements of the BVIF slow down. The Type III BVIF is ideally capable of yielding more than half of its stored energy to the load during such an operation.

4. Prototype testing in the Type III mode has produced real-world evidence of Type III BVIF capacity. Further work remains to be done to fully characterize the nature of such systems.

5. Throughout this study the BVIF was treated only in the mode of giving up stored energy. A study is needed on the effects of BVIF design parameters and load conditions on the energy absorption or storage mode.

6. The next step in BVIF development is to integrate it into a system with a prime mover. The BVIF with its accelerating capability seems a good choice for hybridizing with a prime mover to add additional power during

acceleration and absorbing power during braking.

REFERENCES

1. Ullman, D.G., "A Variable-Inertia Flywheel As an Energy Storage System", Ph.D. Disseration, Ohio State University, March 1978.

2. Ullman, D.G. and Volkoff, H., "An Introduction to the Variable-Inertia Flywheel (VIF)", Journal of Applied Mechanics, Vol. 46, No.1 March 1979.

3. Ullman, D.G., "Preliminary Development of the Band-Type Variable-Inertia Flywheel (BVIF)", Sandia Laboratories, Albequerque, N.M., (SAND 79-7089), November 1979.

4. Ullman, D.G., and Corey, J., "Second-Stage Development of the Band-Type Variable-Inertia Flywheel", to be published by L.L.L., 1980.

5. Merritt, H.E., "Gear Trains," Pitman and Sons, Ltd., London, England, 1947.

6. Beachley, N.H., and Frank, A.A., "Increased Fuel Economy in Transportation Systems by Use of Energy Management-Second Series Program," D.O.T., December 1975.

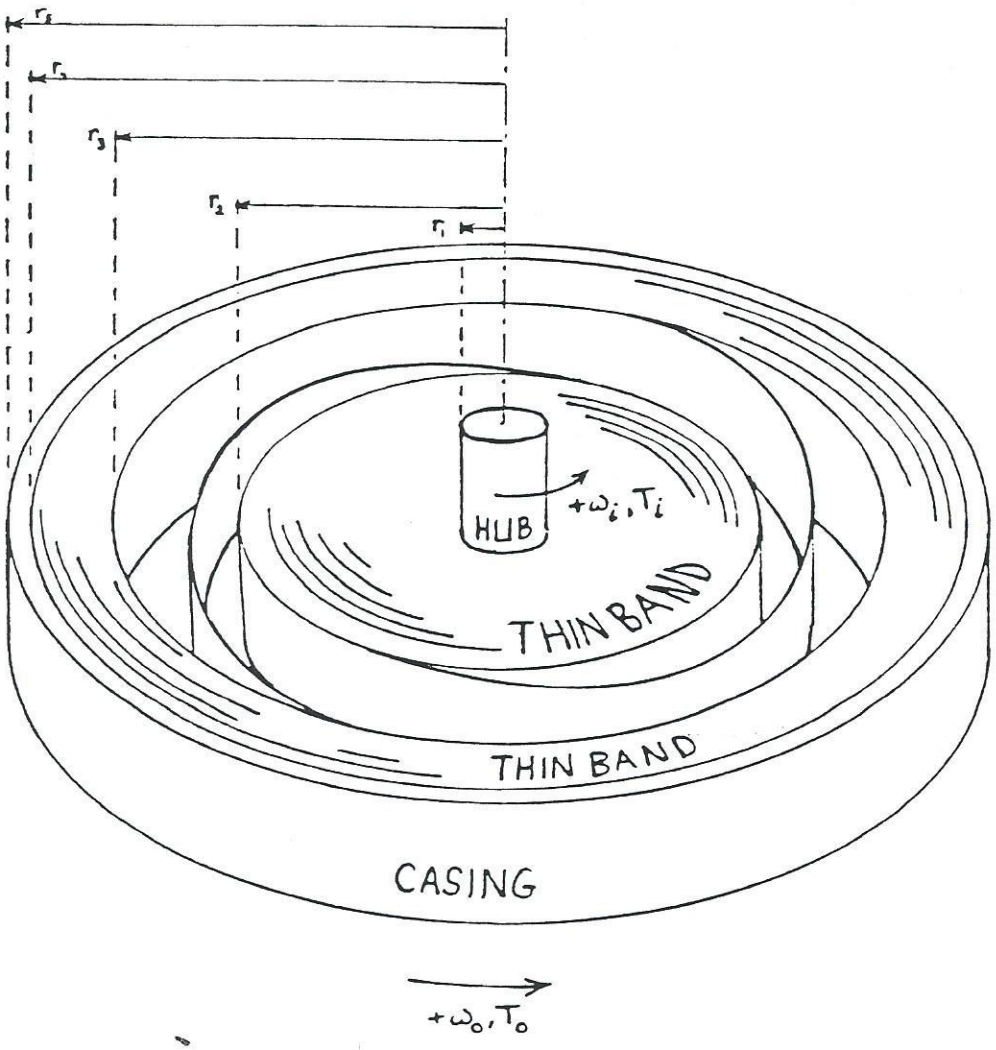

FIGURE 1

BVIF GEOMETRY WITH SIGN CONVENTIONS

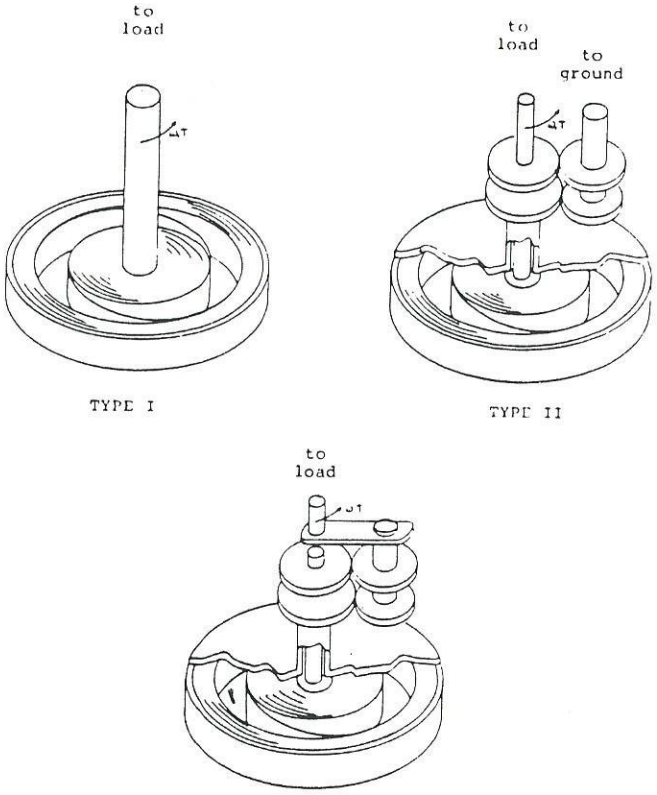

TYPE I

TYPE II

TYPE III

FIGURE 2

BVIF CONFIGURATIONS

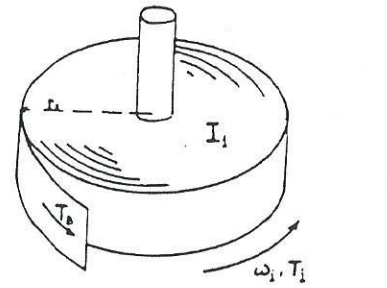

INNER INERTIA FREE-BODY DIAGRAM

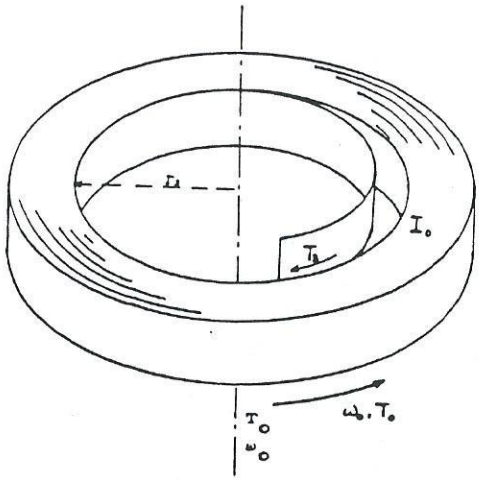

OUTER INERTIA FREE-BODY DIAGRAM

FIGURE 3

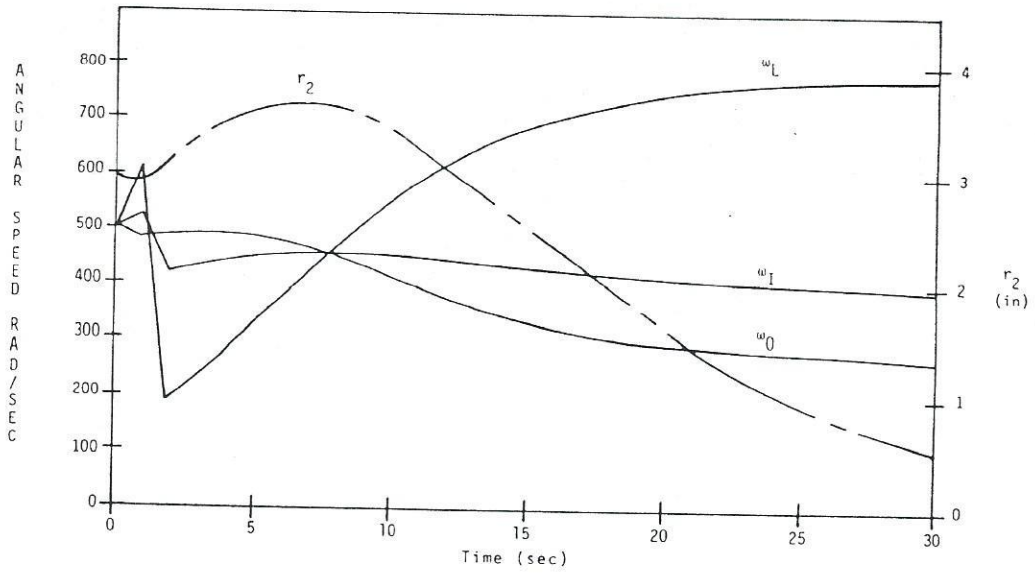

Figure 4a. Type III BVIF Simulation: Angular Rates and Band Position. Time History.

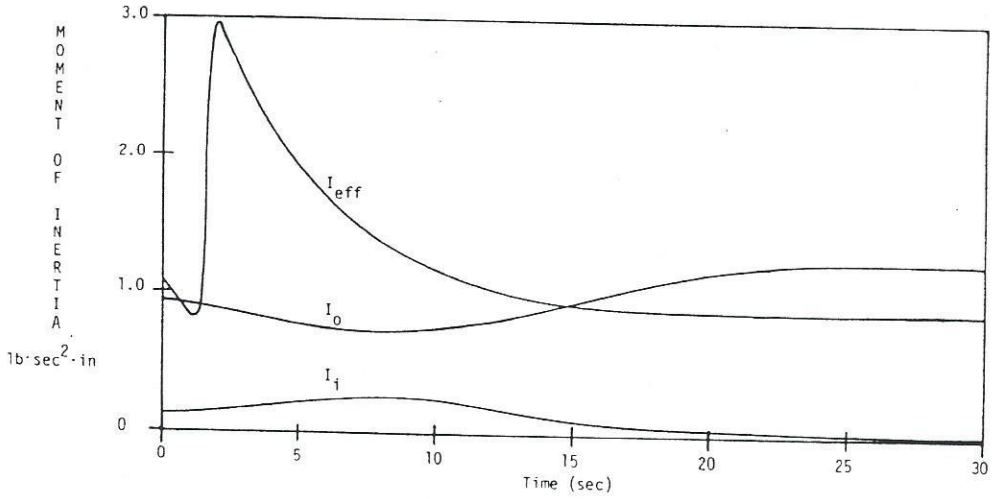

Figure 4b. Type III BVIF Simulation: Moments of Inertia. Time History.

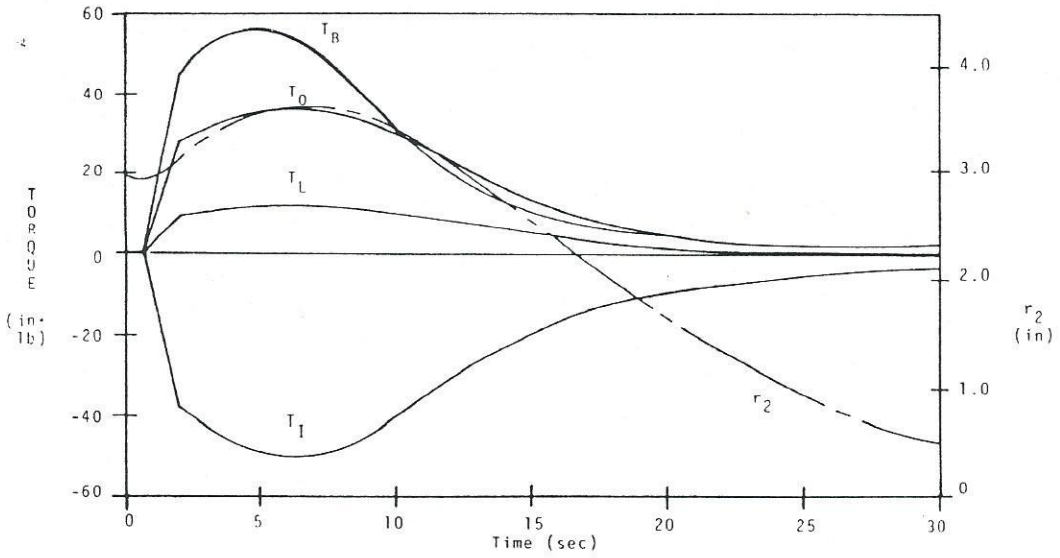

Figure 4c. Type III BVIF Simulation: Torque. Time History.

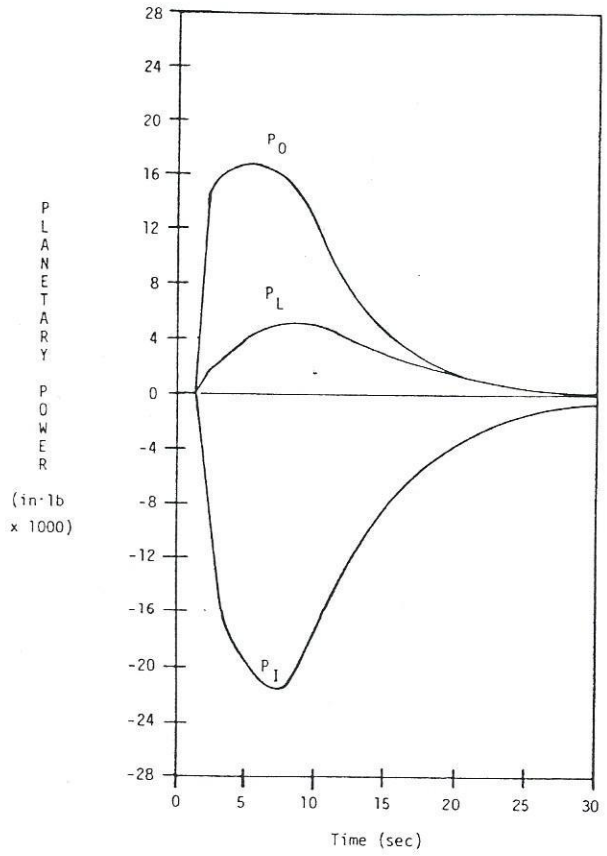

Figure 4d. Type III BVIF Simulation: Planetary Power.

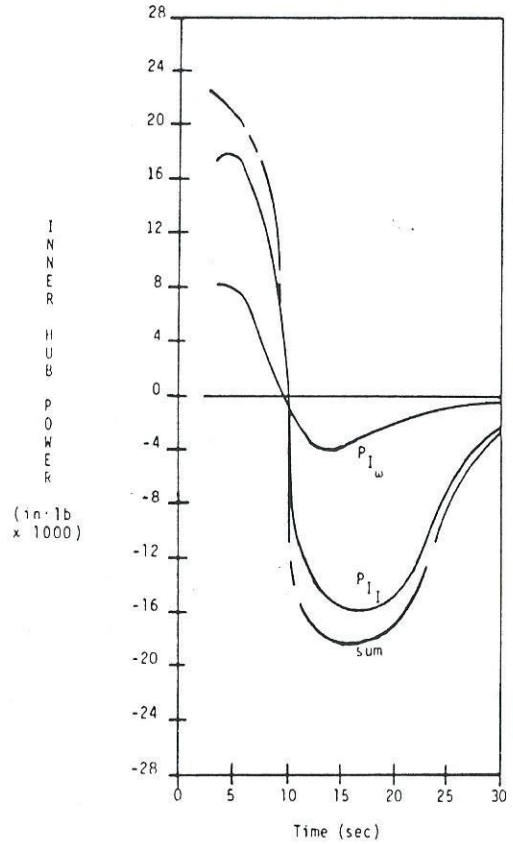

Figure 4e. Type III BVIF: Inner Hub Power. Time History; Plotted After Completed Clutch Engagement for Clarity.

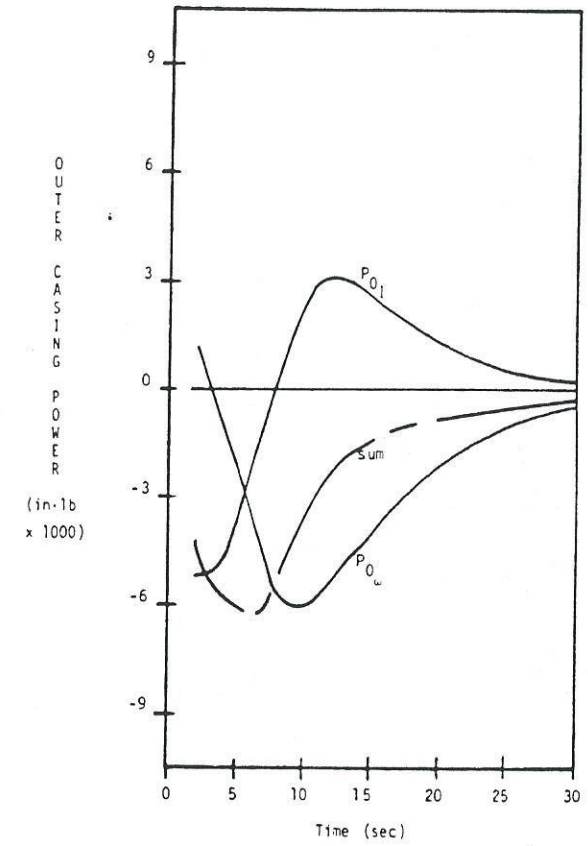

Figure 4f. Type III BVIF Simulation: Outer Casing Power. Time History; Plotted After Completed Clutch Engagement for Clarity.

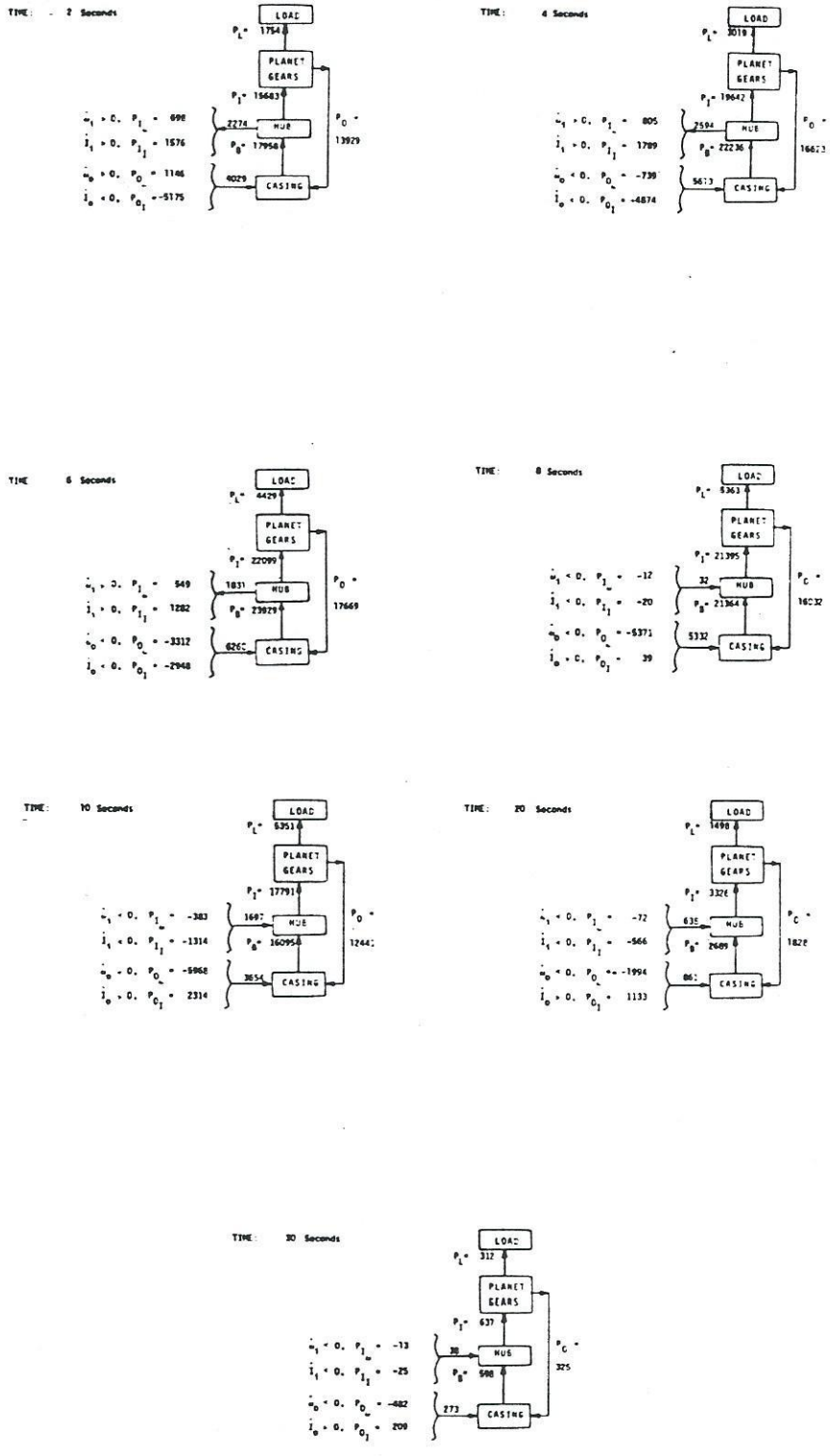

FIGURE 5

POWER FLOW IN BVIF EXAMPLE

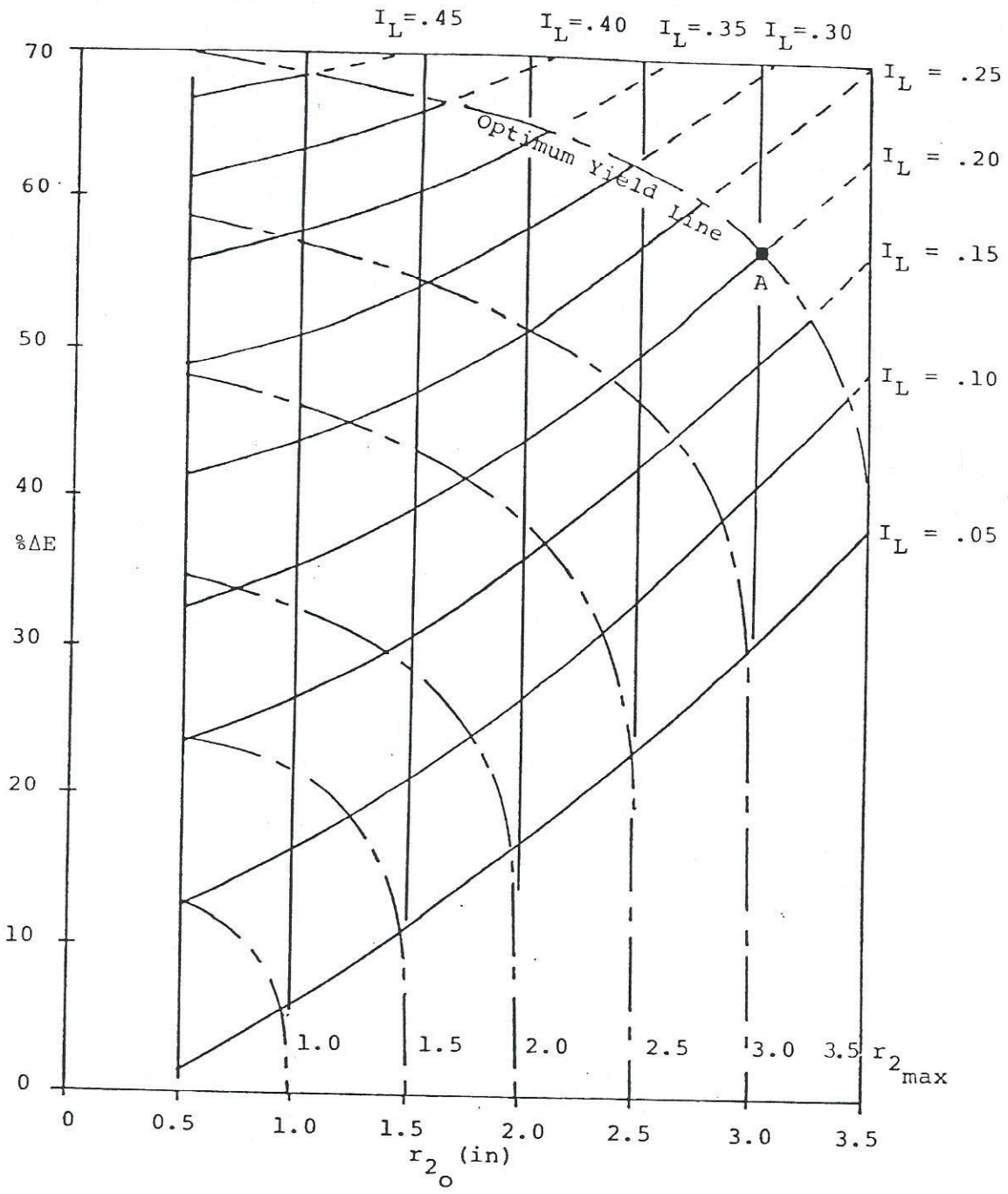

FIGURE 6

FRACTIONAL ENERGY YIELD VS r_{2_o} : Type III BVIF FOR 8 VALUES OF LOAD INERTIA, I_L WITH LINES OF MAXIMUM BAND WIND.

I_L INCLUDES FIXED LOAD SHAFT INERTIA = .05

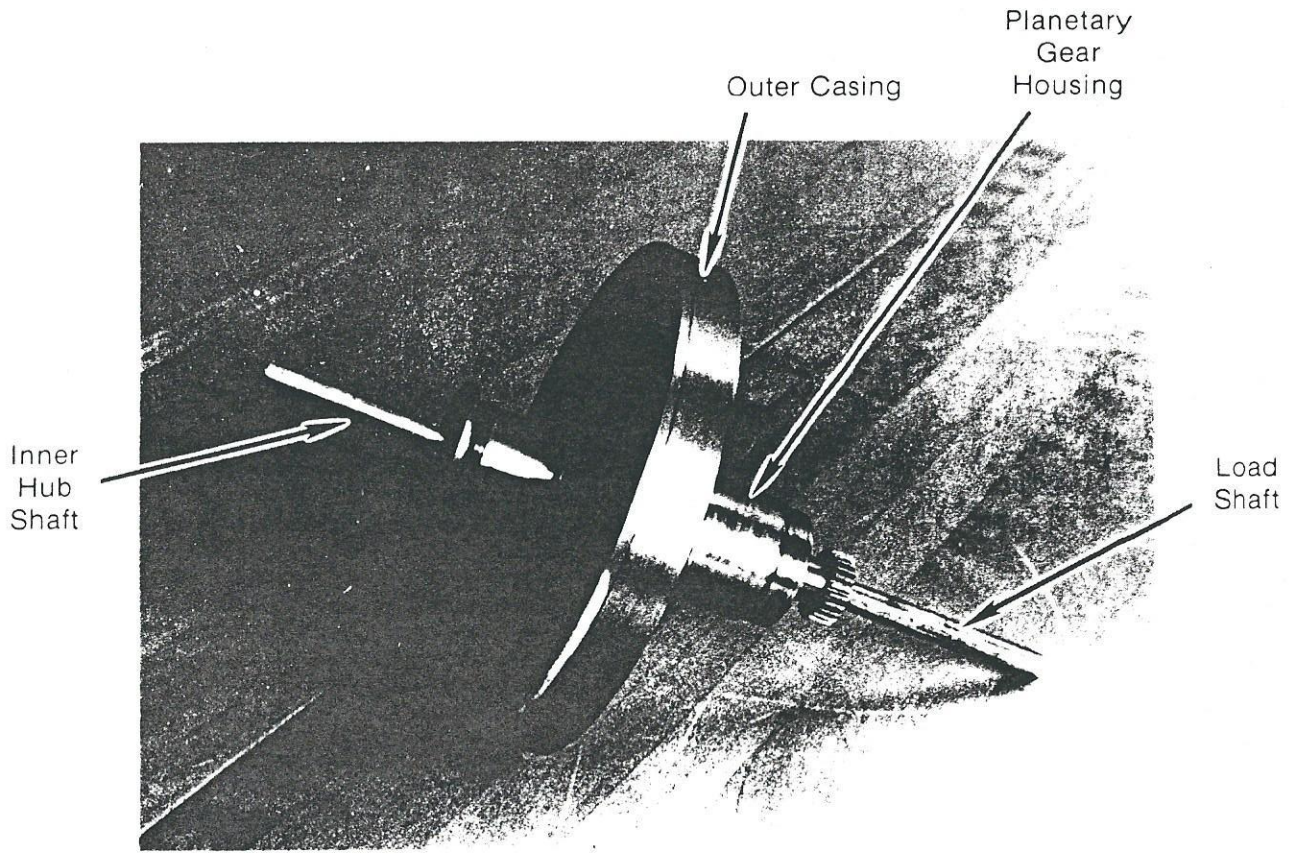

FIGURE 7

PROTOTYPE BVIF

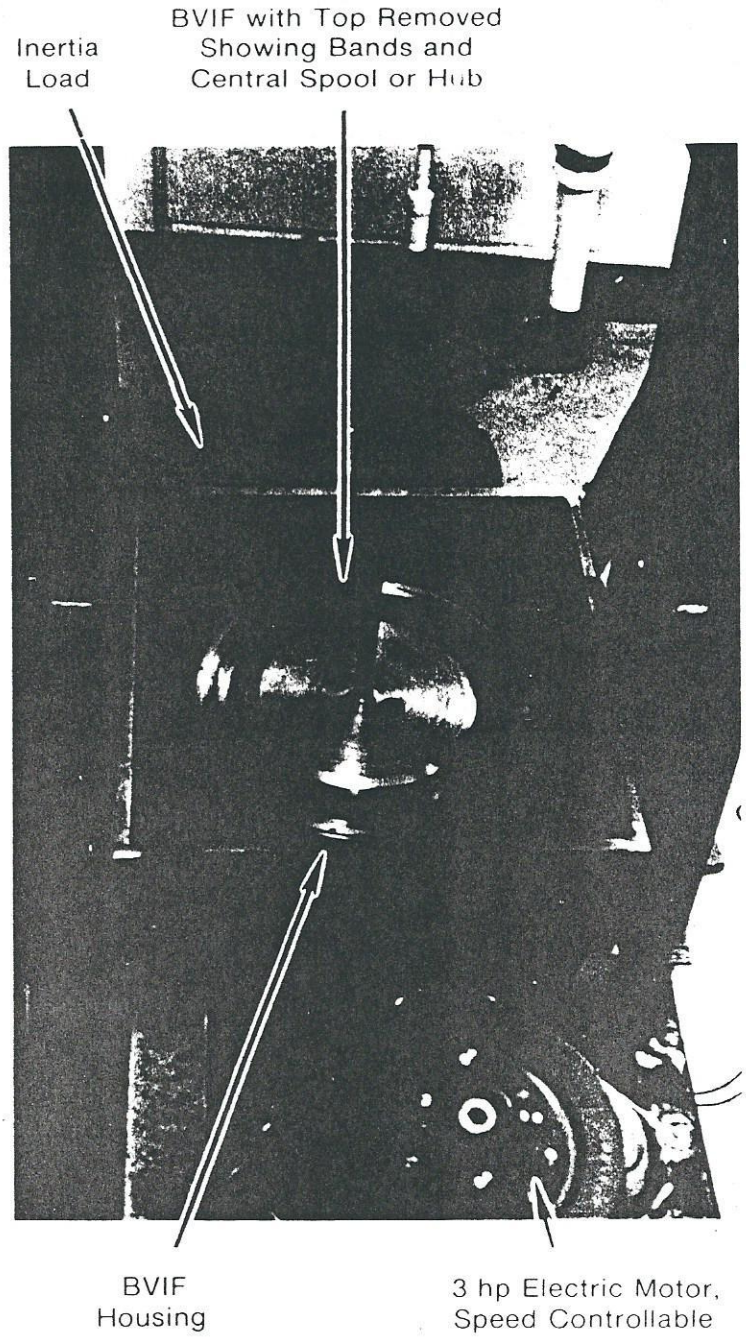

FIGURE 8
BVIF TEST STAND

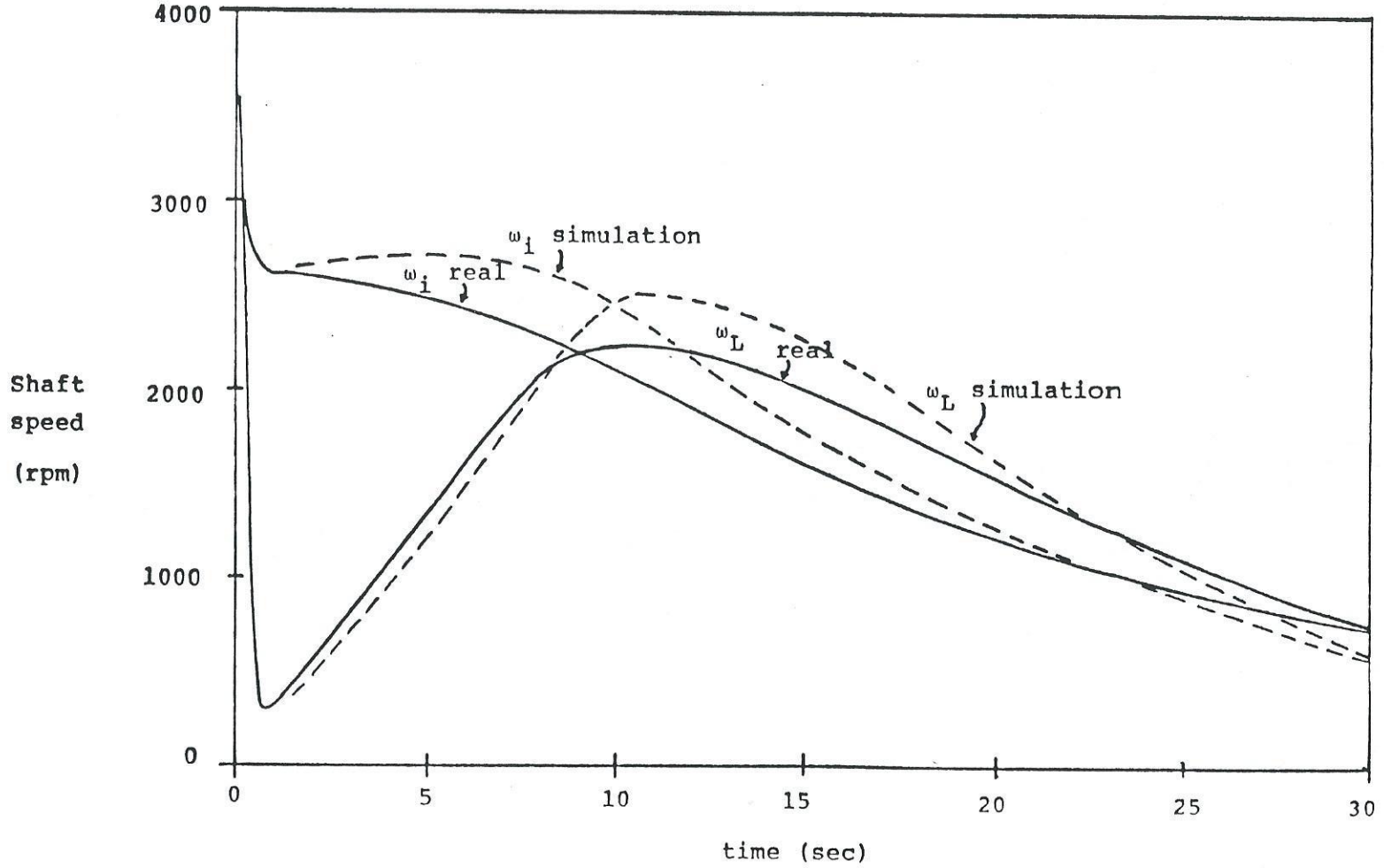

FIGURE 9

COMPARISON OF TYPE III MODEL WITH LOSSES TO ACTUAL PROTOTYPE RUN HISTORY

CONF-801022

1980 FLYWHEEL TECHNOLOGY SYMPOSIUM

October, 1980
Scottsdale, Arizona

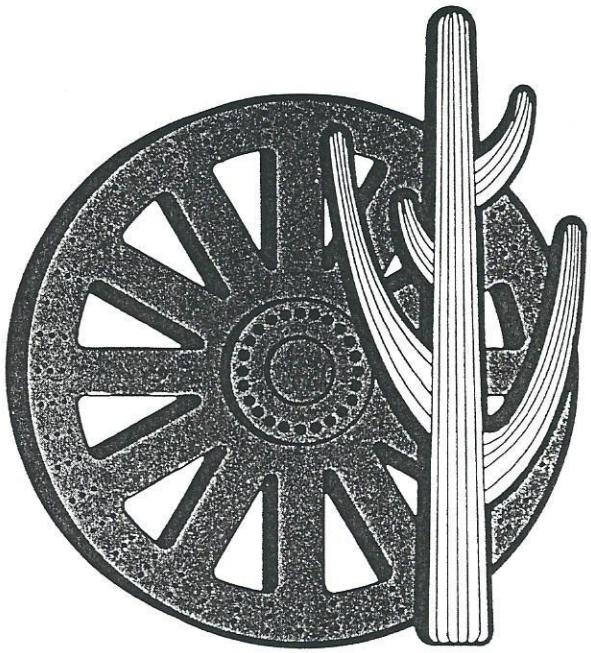

Co-sponsored by
The U.S. Department of Energy

The American Society
of Mechanical Engineers (ASME)

The Lawrence Livermore
National Laboratory